International Journal of Pharmaceutics 418 (2011) 286–296

Contents lists available at ScienceDirect

International Journal of Pharmaceutics

journal homepage: www.elsevier.com/locate/ijpharm

Experiments and numerical modeling to estimate the coating variability in a pan coater

Ekneet Sahni [a], Bodhisattwa Chaudhuri [a,b,*]

[a] Department of Pharmaceutical Sciences, University of Connecticut, Storrs, CT 06269, United States
[b] Institute of Material Sciences, University of Connecticut, Storrs, CT 06269, United States

ARTICLE INFO

Article history:
Received 15 December 2010
Received in revised form 27 April 2011
Accepted 14 May 2011
Available online 20 May 2011

Keywords:
DEM
Pan coating
Coating variability
Frequency distribution

ABSTRACT

The purpose of this work is to investigate the effect of the coating process parameters on coating performance and coating variability, and hence determine the optimal operating conditions. Coating of particles is done to mask the unpleasant taste or odor of the drug, to control the bioavailability of the API, and to increase shelf-life. The coating solution is sprayed in specific locations of the granular bed and coating uniformity is achieved by interparticle collisions and overall mixing behavior in the coater. Thus, good understanding of particle flow and granular mixing in a pan coater is vital to optimize the process parameters to reduce coating variability. Coating experiments are performed at previously determined optimal mixing conditions using Lactose nonpareils. The coating fluid (aqueous solution of Opadry II) is sprayed intermittently at different flow rates and concentration. Vernier Caliper is used to measure the change in diameter and the coating of the particles. Moreover, DEM based numerical modeling of spray coating is also performed for same operational parameter set and spray characteristic (center and the radius of the spray zone) used in the experiments. DEM simulation provides the residence time distribution of all the particles passing through the spray zone. The coating variability in the experiments is estimated at different pan and spray variables. The coating variability decreases with the increase inpan tilt, coating time and an optimum speed. The spray characteristics does not seem to have much effect on the variability although better coating is observed under better mixing conditions of high tilt and pan speed for the same spray parameters. The mass distribution of coated particles is quantified in the numerical model by the total number of particles passing through the spray zone and also by the frequency distribution of the residence time of the coated particles. It is observed that the simulations are in good agreement with the experiments for the effect of orientation (tilt) of the pan coater on coating variability. However simulations over predicted the effect of speed as compared to the experiments to reach the minimum coating variability. In the current study, the experimental setup did not reflect the typical bead coating setup used in the industry; rather depict a simplified setup to validate the numerical model.

1. Introduction

Granular coating is a crucial unit operation in pharmaceutical manufacturing that controls the aesthetics of the final dosage form and has a great impact on the stability of the active drug along with the release profile. Understanding the coating processes takes into account the dynamics of the tablet movement and spray variables (Leaver et al., 1985; Chang and Leonzio, 1995; Fourman et al., 1995) as well as their impact on coating uniformity, functionality, and hence process efficiency.

Coating uniformity was evaluated by calculating the %CV where the difference in the weight gain is calculated by deviation in the amount of the coating received per particle as it passes through the spray. Wide variations in the coating thickness per particle within a batch may have a major impact on coating uniformity particularly if the main purpose is to influence the drug release. Hence, if less amount of coating is obtained, it may cause dose dumping. Conversely, if a particle receives an excess amount of coating material, the drug release is hindered and the onset of action is delayed which may sometimes defeat the purpose of medication. Consequently, a good understanding of the particle dynamics leads to the reduction of the processing time and higher manufacturing efficiency.

A schematic of a pan coater is shown in Fig. 1. The coating solution was sprayed in a moving granular bed with the concurrent

Abbreviations: CV, coefficient of variation; DEM, discrete element method; FR, flow rate; rpm, revolution per minute.

* Corresponding author at: Department of Pharmaceutical Sciences, University of Connecticut, Storrs, CT 06269, United States. Tel.: +1 860 486 4861; fax: +1 860 486 2076.
E-mail address: bodhi.chaudhuri@uconn.edu (B. Chaudhuri).

0378-5173/$ – see front matter © 2011 Elsevier B.V. All rights reserved.
doi:10.1016/j.ijpharm.2011.05.041

Nomenclature

C_i	Concentration of red beads
$\bar{C}$	Average concentration of red beads
d_i	Diameter of the particle
e	Coefficient of restitution
F_i	Total force acting on the particle (N)
F_N	Normal force (N)
F_T	Tangential force (N)
g	Acceleration due to gravity (m/s^2)
I	Intensity of segregation
K_1	Stiffness constant for loading (N/m)
K_2	Stiffness constant for unloading (N/m)
k_T	Tangential stiffness constant (N/m)
m_i	Mass of the particle (kg)
r	Radius of the particle (m)
Δs	Relative tangential displacement between two time steps
T_i	Total tangential force acting on the particle (N)

Greek symbols

α_1	Normal displacement (m)
α_0	Normal displacement when unloading comes to zero (m)
μ	Mean of particle diameter
σ	Standard deviation of particle diameter

use of heated air to facilitate the evaporation of the solvent. As the coater rotates, mixing takes place in the tablet bed as solid body rotation while some particles cascade on the surface. The bed is divided into two regimes in a pan coater: (i) cascading layer composed of a thin layer of particles that flows down the free surface and (ii) quasi-static zone, comprising of remaining particles that rotate as a fixed bed. The regularity with which the particles pass through the spray zone plays an important role in determining the overall coating uniformity of the batch. During coating the time for which the particles reside at the surface of the cascading bed (i.e. residence time) determines how much spray an individual particle receives per pass through the spray zone. The coating variability is therefore dependent on the particle's residence time.

Qualitative information regarding the effect of speed on residence times and coating duration on coating variability is available in the literature. Many studies in literature have reported that the residence time under the spray decreases as the pan rotational speed and the fill load were increases (Prater et al., 1980; Yamane et al., 1995; Tobiska and Kleinebudde, 2001; Sandadi et al., 2004). In contrast, Kalbag et al. (2008) and Denis et al. (2003) suggested that the pan load does not affect the average residence time per pass. Studies by Leaver et al. (1985) suggested that the inter-tablet variability decreases with increased drum speed and fill level. In contrast, Chang and Leonzio (1995) did not observe any distinct trends regarding the drum speed and the inter-tablet variability, which according to them is due to the spray drying and coat transfer effects.

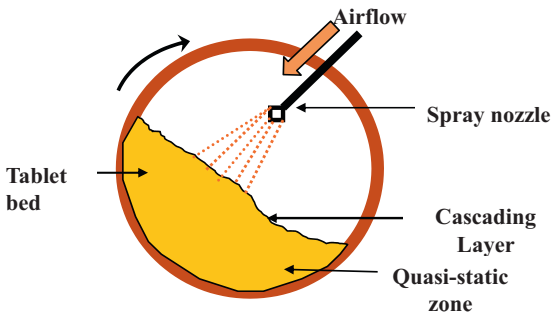

Fig. 1. Schematic of the pan coater showing quasi-static and cascading zones in the bed as the coater rotates.

Not much work has been done quantifying the effect of spray characteristics on coating variability. Skultety et al. (1988) reported that wide, uniform spray pattern significantly decreases the inter-tablet coating variability when compared to the narrow spray pattern. They also illustrated that higher spray rates resulted in greater coating variability although, the related variability coefficients were not discussed. Tobiska and Kleinebudde (2001) observed that the coating variability increased with an increase in spray rates at low pan speeds. To the best of our knowledge, no experimentally validated numerical modeling studies concentrate on the effect of high vessel speeds at higher spray rates and spray fluid concentration on coating performance.

Till date only a few studies in literature have focused on coating variability. Turton (2008) adopted different modeling approaches to estimate the weight gain variabilityin a pan coater. Mann (1983) predicted the coefficient of variation in a spouted bed describing the dependence of variability on circulation time, average weight gain and their distributions using the renewal theory model. Population balance approach was also used in predicting the coefficient of variation in a fluidized bed (Sherony, 1981) and for simulating the pan coating operation (Denis et al., 2003). However, this approach limits the model parameters and hence the practical applicability of the model itself. Pan coating simulation based on Continuum approach developed by Khakhar et al. (1997) illustrated that the behavior of the material is described by the complex constitutive equations, which fail to account for real material properties.

Substantial work has also been done using Monte Carlo simulations on coating and granulation of particles (Kushaari et al., 2006) as well as to compute the coating mass distribution in a tumbling fluidized bed coater (Nakamura et al., 1998). Pandey et al. (2006a,b) used the Monte Carlo simulations to relate the probability distribution of events in a pan coater with the process variables which affect the mass coating variability. In addition, a mathematical model has been developed by Joglekar et al. (2007) to estimate the weight gain variability in a pan coater with the following oversimplified assumptions: (1) presence of constant number of tablets in coating zone and (2) equal residence time for the tablet within the spray zone. In all of the above mentioned modeling approaches, model parameters must either be measured separately by performing extensive experimental analysis or were simply adjusted to give a good agreement. Hence, *a priori* prediction is not possible because of their descriptive nature.

On the other hand, Discrete Element Method (DEM), proposed by Strack and Cundall (1979) is a deterministic approach to investigate the particle dynamics. It is used in several operations involved in process industry and in particle coating application; Mishra and Rajamani (1992), Walton and Braun (1993), Yamane et al. (1995) and Pandey et al. (2006a,b). Inter and intra tablet coating variability in a pan coater has been studied using DEM and Monte Carlo based simulations (Kalbag et al., 2008; Kalbag and Wassgren, 2009). DEM predicts the evolution of trajectories of individual particles of granular media using Newton's equations of motion, hence deriving the necessary information about position and velocity profiles of the discrete particle. Particle properties such as size, density, spring constants, Young's modulus, and Poisson's ratio (Rothenburg and Bathurst, 1992) can be incorporated into the DEM model to realistically model the granular flow. Hence, in the view of published studies and often-inconsistent observations, a systematic and comprehensive analysis of pan and spray variables affecting the coating process is performed.

Table 1
The parameters employed in the DEM simulations.

Parameters	Values
Total number of particles	40,000–90,000
Radius of the particles	1.7 mm
Density of the particles	1.6 g/cm^3
Frictional coefficients	
Particle/particle	0.7
Particle/wall	0.4
Coefficient of restitution	
Particle/particle	0.7
Particle/wall	0.5
Normal stiffness coefficient	
Particle/particle	6000 N/m
Particle/wall	6000 N/m
Time step (Δt)	2.0×10^{-6} s

Although pan coaters are extensively used because of their simple operation but they often suffer from high product variability. Therefore, in order to ensure the coating uniformity, the current study aims at understanding and investigating the variables affecting coating uniformity in a pan coating process. Furthermore, a three-dimensional DEM model was developed to predict the residence time distribution of the particles in the spray zone.

2. Materials and methods

2.1. Experimental setup

2.1.1. Materials

The coating study was performed on white colored Lactose non-pareils obtained from Paulaur Corporation (Cranbury, NJ) of diameter 3.3–3.5 mm. The non-pareils was selected as a model compound because spherical particles with well-known physical properties (stated in Table 1) were preferred to conveniently compare with the simulation results of the DEM model (which simply deals with the spherical particles). The non-pareils were coated upto 6% theoretical weight gain using Black Opadry II (Composition: Polyethylene glycol and Talc) obtained from Colorcon (West Point, PA). Opadry II has the capability to be applied at high solids concentration and still 'maintaining the low viscosity. The aqueous coating solution was prepared at various solids concentration. Non-pareils and particles are used interchangeably in the text.

2.1.2. Apparatus

The coating experiments were conducted in an oblate spheroid shaped pan coater (Erweka, Germany, diameter 0.38 m) as shown in Fig. 2a, the drive mechanism of which is computer controlled. A combination of peristaltic pump, a fluid-flow controller and an atomizing nozzle (Cole Palmer, IL) was used as the spray system as indicated in Fig. 2a.

Optimal mixing condition was determined (Sahni et al., 2011) where the granular mixing experiments were carried out with white and red colored lactose non-pareils. Initially the coater was loaded with white and red colored lactose non-pareils in a completely segregated manner and subsequently the coater was rotated to mix them. The pan coater was stopped at definite time intervals for sampling. A discrete pocket sampler (Ere Inc., Montreal), an intrusive sampling technique (shown in Fig. 2b) was used for sampling non-pareils at definite time intervals. It was further facilitated by another custom made cardboard template with four ports for sample extraction as shown in the Fig. 2c. The template was placed on the top of the granular bed where the template ensured sample extraction from the same position during the course of the experiment. The sampler was inserted in its opened position through the sample ports until a particular depth, allowing accumulation of particles followed by locking the sampler to avoid any loss of sample before pulling out of the bed. The sample size comprised of almost 150–200 particles. The concentration of red particles in the sample was determined by manually counting the number of red and white particles at each of the four sample points. Apart from using discrete pocket sampler, video-imaging was also used to quantify mixing. Mixing patterns were examined and mixing performance was characterized in the coating pan for the following set of parameters:

1. *Pan rotational speed*: 10 rpm, 20 rpm, 30 rpm.
2. *Pan fill level*: 1.5 L, 2.64 L, 3.4 L (21%, 37% and 48%).
3. *Vessel tilt from horizontal*: 0°, 16°, 32°.

The extent of mixing was characterized by the intensity of segregation parameter I, defined as the ratio of variance at any time to the same at time = 0 s and calculated as:

$$I = \frac{\sigma^2}{\sigma_0^2} \quad (1)$$

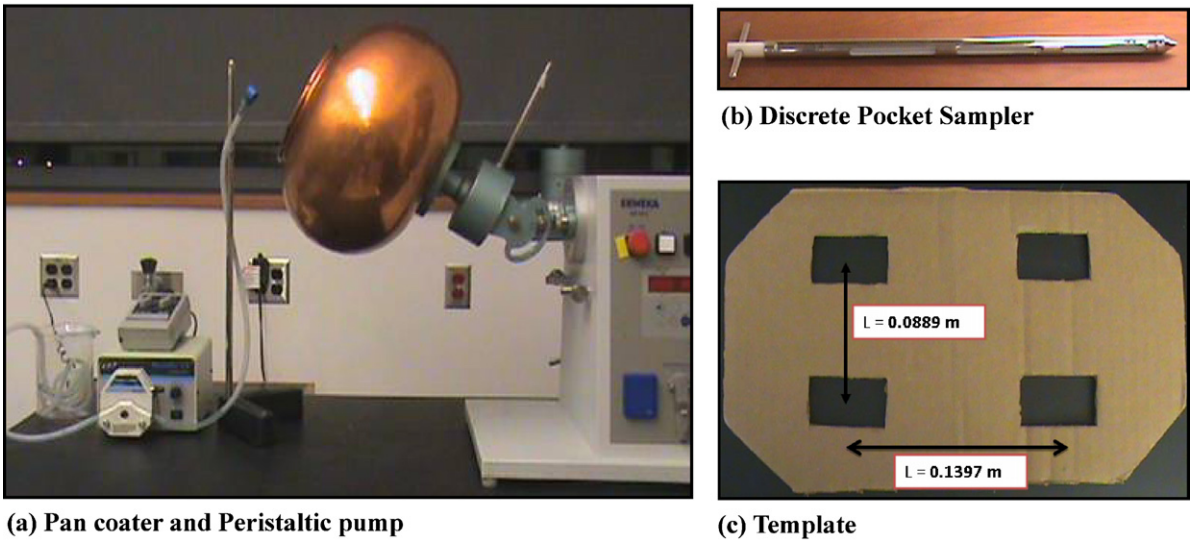

Fig. 2. (a) Experimental set up for coating of non-pareils, including the oblate spheroid shaped pan coater and digitally controlled peristaltic pump. (b) Discrete pocket sampler used to characterize the spatial distribution of the colored nonpareils as a function of time for several values of vessel speed and fill level. (c) Shows a self constructed template with four ports through which the discrete pocket sampler is inserted for sample extraction.

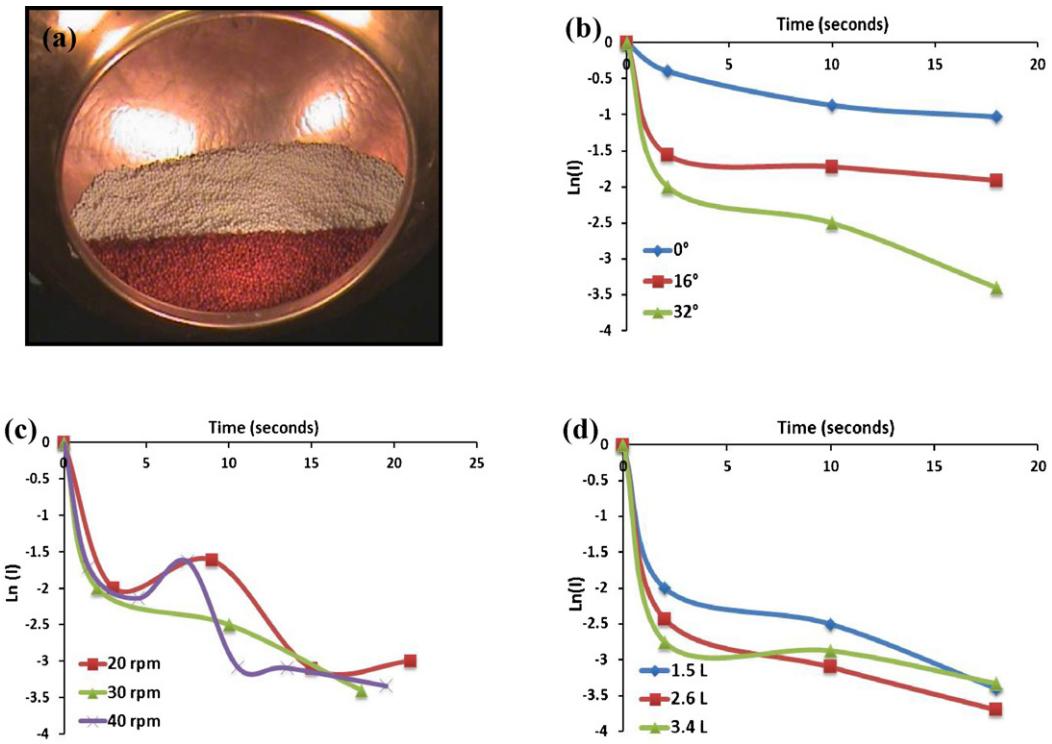

Fig. 3. (a) The initial setup of the mixing experiment where white and red non pareils were loaded in front-back manner. (b) Variation of intensity of segregation with time as a function of orientation of the pan coater. (c) Variation of intensity of segregation with time as a function of the speed of the vessel. (d) Temporal variation of intensity of segregation as function of fill fraction of the pan coater.

where

$$\sigma^2 = \frac{\sum(C_i - \bar{C})^2}{N} \quad (2)$$

where C_i is the concentration of red non-pareils at point i (i corresponds to the sample points, $i = 1, 2, 3, 4$), $\bar{C}$ the average concentration of red non-pareils and N the number of sample points ($N = 4$).

Intensity of segregation was estimated from the sample data collected at different time intervals. Fig. 3b illustrates the variation of intensity of segregation of red non-pareils with time at three different orientations (0°,16°, and 32°with the horizontal axis) of the coater. The decrease in segregation occurs faster with an optimum increase in the angle of the coater with the horizontal. Moreover, the rotational speed and fill ratio of the vessel do not have much effect on the intensity of segregation as shown in Fig. 3c and d, respectively. DEM based numerical model (as elaborated in Sahni et al., 2011) was also developed to study the effect of granular mixing in the pan coater where simulations derive essentially the same conclusions as that of the experiments.

2.1.3. Protocol for coating experiments

In the current study, the experimental setup did not reflect the typical bead coating setup used in the industry; rather depict a simplified setup to validate the numerical model. In order to characterize the coating variability, the experiments were performed using a conventional pan coater under optimal mixing conditions of 21% fill fraction, 32° orientation, and pan speed of 30 rpm using white colored lactose non-pareils (3.3–3.5 mm). An aqueous solution of different concentrations of Opadry II was prepared. The pan was loaded with lactose non-pareils where the bed was initially warmed at ~50 °C. For each experimental study, the bed was heated using an industrial heater, placed at the opening of the coater to enhance the drying of the bed and prevent sticking when coating solution was being applied to the granular bed. The coater was stopped and samples were withdrawn at specific time intervals using a discrete pocket sampler and a sampling template as described above. The spraying of coating fluid was done intermittently until the bed was uniformly coated. The coating time for all experimental runs was 20 min.

A Vernier Caliper with a precision of 0.01 mmwas used to measure the change in the particle diameter during coating. Vernier caliper was used, as it is a direct means of measurement for measuring average coating thickness of ~3–6% (which corresponds to ~100–250 μm). The withdrawn samples were dried in the oven at 85 °C. The average diameter and the standard deviation of coated particles for all the samples were calculated to compute the coating variability for following set of operational parameters:

1. *Spray flow rate*: 0.486 mL/min, 1.653 mL/min, and 2.316 mL/min.
2. *Spray fluid concentration*: 5%, 10%, and 20%.
3. *Vessel tilt*: 0°, 16°, 32° and 45°.
4. *Vessel speed*: 5 rpm, 10 rpm, 20 rpm, and 30 rpm.

2.2. Simulation method

In the present study, a three-dimensional, soft-particle, previously developed DEM (Moakher et al., 2000) program was used with appropriate physical properties of the non-pareils to model the particle dynamics in the rotating pan coater.

The numerical model was developed based on the following assumptions:

1. Presence of coating fluid was not considered.
2. Physical properties such as Young's modulus and density were kept constant during the simulation.

As very small amount of coating solution was introduced into the bed which dried immediately, the DEM model developed simply deals with a dry granular bed. Instead, the particles were color-coded based on their residence time under the spray zone for visual purposes.

The particles considered were a collection of frictional and inelastic spheres. The forces and torques acting on each of the particles was calculated in the following way:

$$\Sigma F_i = m_i g + F_N + F_T \quad (3)$$

$$\Sigma T_i = r_i \times F_T \quad (4)$$

The force on each particle was given by the sum of gravitational and inter-particle (normal and tangential F_N and F_T) collisional forces as indicated in Eq. (3). The corresponding torque on each particle was the sum of the moment of the tangential forces (F_T) arising from inter-particle contacts (Eq. (4)).

The normal force was calculated using the "latching spring model", developed by Walton and Braun (1986, 1993), which allows colliding particles to overlap. Each particle may interact with its neighbors or with the boundary only at contact points through the normal and the tangential forces. The normal forces between pairs of particles in contact was defined using a spring with constants K_1 and K_2 for compression and recovery: $F_N = K_1\alpha_1$ (for compression), and $F_N = K_2(\alpha_1 - \alpha_0)$ (for recovery). These spring constants K_1 and K_2 were chosen to be large enough to ensure that the overlaps α_1 and α_0 remain small compared to the particles sizes. The degree of inelasticity of collisions was incorporated in this model by including a coefficient of restitution $e = (K_1/K_2)^{1/2}$ ($0 < e < 1$, where $e = 1$ implies a perfectly elastic collision with no energy dissipation, $e = 0$ implies a completely inelastic collision).

Tangential force (F_T) in inter-particle or particle-wall collision was calculated employing Walton's incrementally slipping friction model (Walton and Braun, 1986, 1993). After the contact occurs, the tangential forces buildup, causing displacement in the tangential plane of contact. The tangential force F_T was evaluated considering an effective tangential stiffness k_T associated with a linear spring. It incremented at each time step as $F_{Tt+1} = F_{Tt} + k_T\Delta s$, where Δs is the relative tangential displacement between two time steps.

DEM simulations provide the temporal variation of velocity, orientation, and position of each particle within the coater, allowing true measurements of the time that each particle spends in the spray zone. The particles were assigned random initial non overlapping positions and then allowed to settle inside the coater under the force of gravity. This initial configuration was equilibrated for a period of five seconds and then the coater boundary begins to rotate at a fixed revolution per minute (rpm) value. 40,000–100,000 spherical inelastic frictional particles were initially loaded within the pan coater based on different fill levels. In DEM as the 3D position of every particle was known, it was easy to perform sampling of particles from specified locations and then counting the number of each species. A circular spray zone on the surface of the granular bed was assumed similar to that of coating experiments. The three dimensional coordinate of the center of the spray and the radius of the spray zone on the granular bed ascertained from the experiments as mentioned earlier was used to determine the residence time distribution of all the particles in the bed from the particle trajectory produced by the simulation. The coating variability was therefore dependent on the residence time spent by the non-pareils under the spray zone. Any variation in residence time was reflected as variation in the coating distribution of a coated batch of particles. Simulation of coating process was achieved by post processing the particle dynamics data.

DEM simulations were performed using 40,000 particles (corresponding to 21% fill fraction) where the spray duration was 1 s and the time difference between the initial and the next spray was 3 s. This ratio was similar to the ratio of spray time and difference between two sprays in the experiments. The residence time for each particle was subsequently estimated. The particles were color coded for viewing based on the residence time in the spray zone for the interpretation of coating in the simulation. Quantities estimated in each run of the parametric study include:

1. Total number of particles passed through the spray zone.
2. Frequency distribution of the residence time of the coated particles.

3. Results and discussion

3.1. Coating variability

Enhanced understanding of the pan coating operation leads to an improved process performance. From the previous coating results (Sahni et al., 2011), we gained that a balance between particle motion, which includes the frequency and duration of particle appearance in the spray zone, and spray variables is essential to achieve optimal coating. The variability in the total mass deposited on the particles is not only due to variation in the quantity of material deposited when the particles pass through the spray zone but also due to the difference in the number of times the same particle is reintroduced into the spray zone (Cheng and Turton, 1999). The particle movement in the pan coater during the coating operation is dependent on various factors, which involve parameters like rotational speed, vessel fill, tilt, and spray variables such as spray concentration, spray flow rate, nozzle to bed distance, and spray area. Due to variations in these process parameters, particles under the spray zone show variation in the residence time leading to coating variability.

Particle to particle coating variability is quantified by measuring the relative standard deviation or by calculating the coefficient of variation (Chang and Leonzio, 1995). The coating variability for lactose non-pareils was therefore calculated using the following relation:

$$\mathrm{CV} = \frac{\sigma}{\mu}$$

where CV is the coating variability (coefficient of variation), σ is the standard deviation of the change in diameter of non-pareils for a particular set of experiment and μ is the average for the same coating distribution. The following relations give standard deviation and average coating weight gain (calculated by increase in diameter) respectively:

$$\sigma = \left\{ \frac{1}{N} \sum_{i=1}^{N} (d_i - \mu)^2 \right\}^{1/2}$$

$$\mu = \frac{1}{N} \sum_{i=1}^{N} d_i$$

where N is the total number of non-pareils in the sample and d_i is the diameter of the ith particle in the sample withdrawn at a particular time interval.

The nozzle to the bed distance and spray area were kept constant for all the experimental runs (Sahni et al., 2011). As the mass coating variability decreased with decrease in pan loading, a lower fill volume of 1.5 L (corresponding to 21% fill) was selected for the experiments (Pandey et al., 2006a,b) to have sufficient particle movement in the bed to ensure an even distribution of the coating spray in the granular bed.

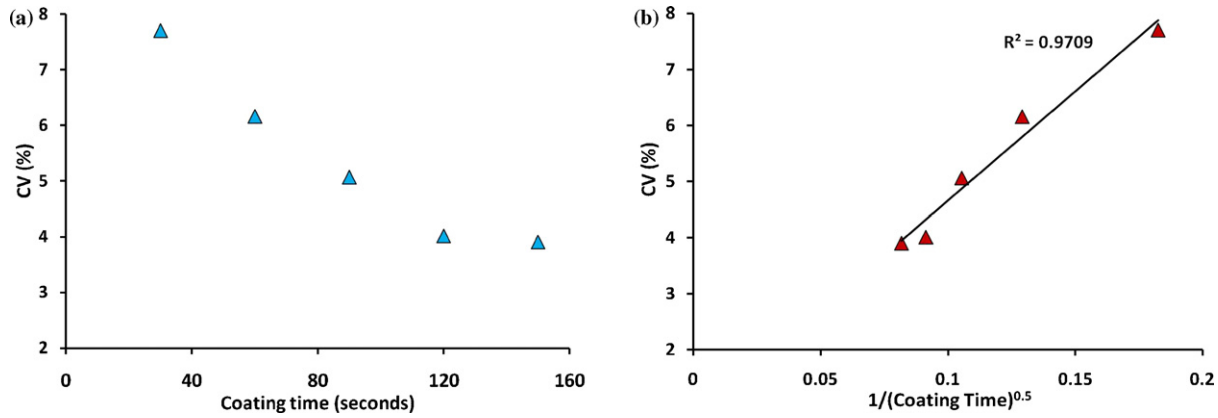

Fig. 4. (a) Effect of coating time on coating variability (CV) at 20 rpm, 21% fill load, 20% Opadry II, and 2.316 mL/min spray rate. (b) Inverse relation of coating variability with square root of time under similar experimental conditions.

3.2. Parameters affecting coating variability

3.2.1. Effect of coating time on coating variability

The effect of coating time on coating variability is illustrated in Figs. 4 and 5 where Figs. 4a and 5a show the variation of the average diameter of the coated particles as a function of elapsed time with 20 and 30 rpm, respectively. The coating experiments were performed at 1.5 L fill, 32° tilt and 2.316 mL/minspray rate using 20% Opadry II. The coated particles encounter the uncoated particles and the variability decreases with the course of time and eventually plateau off. CV is also inversely proportional to the square root of coating time as shown in Figs. 4b and 5b. The variability is higher initially for 20 rpm (7.7%) as compared to 30 rpm (4.96%) but decreased to almost 4% at 120 and 100 seconds with R^2 value as 0.97and 0.82 for 20 and 30 rpm, respectively. These results fit well with the conclusions of Pandey et al. (2006a,b) and many others in literature.

3.2.2. Effect of solid flow rate and spray concentration on coating variability

The spray flow rate and concentration of the atomized coating solution influences the size of the droplet. The atomizing nozzle was fixed at a distance of 6 in. so as to prevent drying of an aqueous solution of Opadry II prior to adhesion to the particles thereby ensuring optimum spray conditions. Fig. 6 shows the effect of solid spray rate on coating variability at 21% (1.5 L) fill fraction at 32° and 30 rpm. The effect of three different flow rates was observed at 20% Opadry II concentration: 0.486 mL/min (Flow rate 1), 1.653 mL/min (Flow rate 3), and 2.316 mL/min (Flow rate 6). Fig. 6a compares the coating variability at the end of coating run for all the flow rates, where the coating variability increased with increase in the flow rate from FR 1 (4.54% variability) to FR 3 (5.32% variability) and then further decreased as flow rate increased to FR 6 (4.12% variability). The increase in variability with flow rate has been observed in literature (Joglekar et al., 2007) because it introduces a higher variability for coating that will be applied on the particle during each coating revolution and between successive coating events. Higher spray rate results in over wetting and hence agglomeration of the particles. On the other hand, too slow a spray causes the coating material to dry resulting in a rough surface and consequently poor coating efficiency.

Therefore, it is clear from the frequency distribution curve in Fig. 6b, that as the particles were coated there was a shift in the diameter of the uncoated particles with increasing flow rate as observed from the bell shaped curve. As the distribution gets wider as for FR 3 as compared to FR 1, the variability was higher for FR 3. FR 6 (4.12% variability) unlike FR 3 shows lesser variability as suggested by a tighter distribution in Fig. 6b. This is possible because of less coating time and therefore fewer inter-particle and particle-wall interactions resulting in faster uniform coating.

The effect of spray concentration on coating variability is illustrated in Fig. 7. The coating experiments were performed at 1.5 L fill, 32° tilt, 30 rpm and 2.316 mL/min spray rate for three different concentrations of aqueous Opadry II: 5%, 10%, and 20%. Fig. 7a shows that there is not much difference in the coating variability at lower concentration but the variability decreased at high concentration of Opadry II. The frequency distribution plots for different Opadry II concentration in Fig. 7b shows a shift in the curve with an

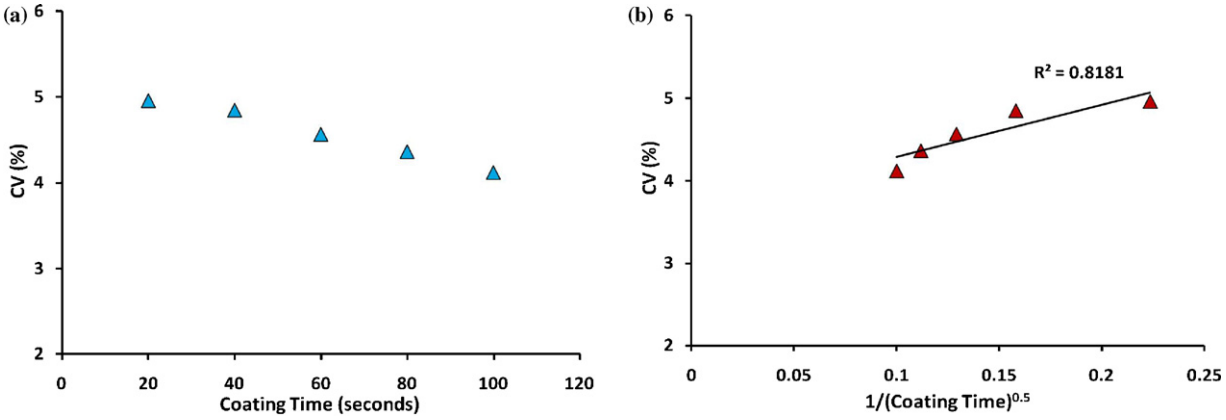

Fig. 5. (a) Effect of coating time on coating variability (CV) at 30 rpm, pan load of 21% fill, 20% Opadry II, and spray rate of 2.316 mL/min. (b) The inverse relation of coating variability with square root of time under comparable experimental conditions.

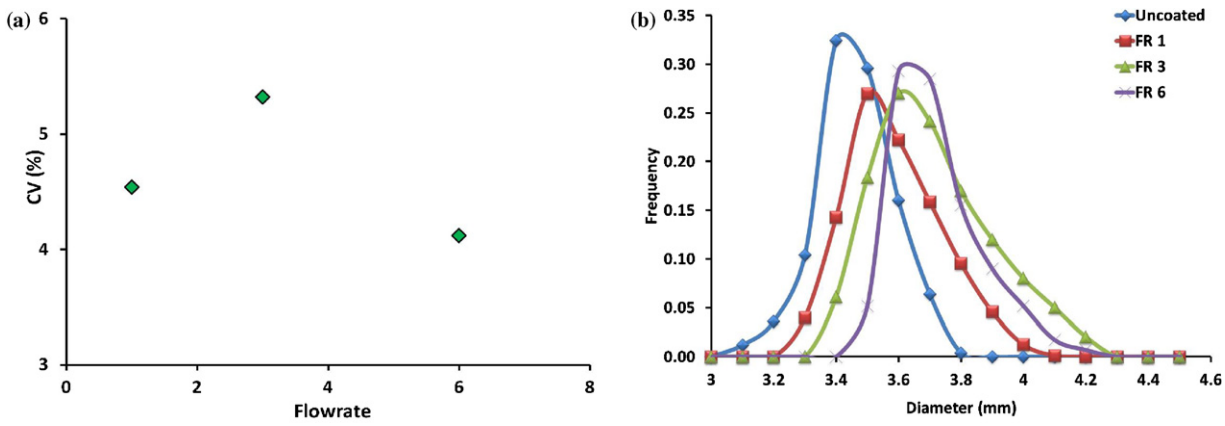

Fig. 6. (a) Effect of three different flow rates at 30 rpm and 20% concentration on CV: flow rate 1 (0.486 mL/min), flow rate 3 (1.653 mL/min), and flow rate 6 (2.316 mL/min). (b) The frequency distribution with respect to the change in diameter of non-pareils under similar conditions.

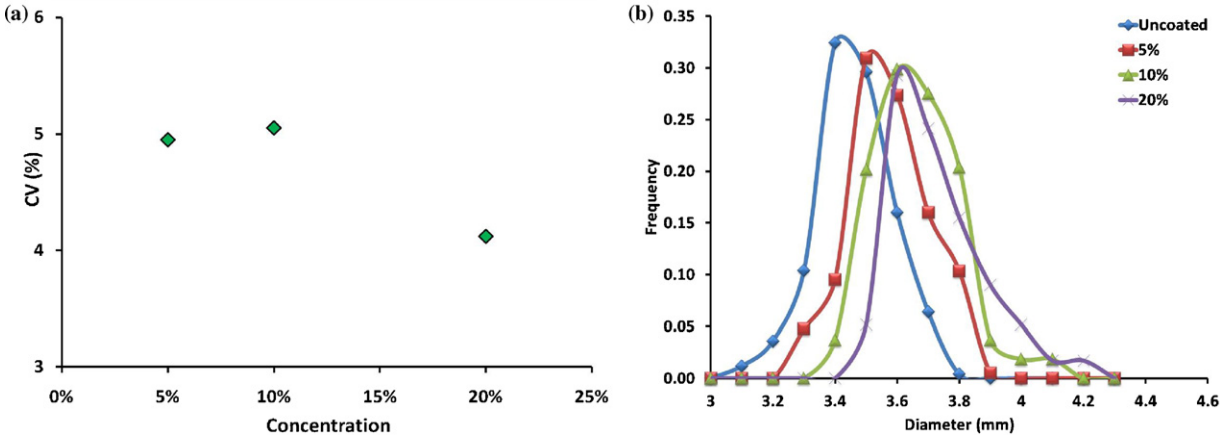

Fig. 7. (a) Effect of three different spray concentration at 30 rpm and FR 6 (2.316 mL/min) on CV: 5%, 15%, and 20%. The frequency distribution with respect to the change in diameter of non-pareils for the effect of spray concentration at pan rotational speed of 30 rpm and FR 6 (2.316 mL/min).

increase in the concentration and hence the diameter. Therefore, a combination of 20% spray concentration and FR6was used for further studies by varying other variables like pan tilt and rotational speed. No simulations were performed to check the effect of flow rate and spray concentration on the coating variability.

3.2.3. *Effect of pan tilt on coating variability*

From the previous studies (Sahni et al., 2011) on mixing, we have learned that the pan tilt enhances axial mixing of the bed resulting in better coating. The effect of different tilts was observed at 1.5 L fill, 30 rpm, 20% solids concentration, and FR 6 (2.316 mL/min). The variability of the coated particles (%CV) was plotted at regular intervals of time as a function of different pan orientations: 0°, 16°, 32°, and 45° as shown in Fig. 8a. The coating variability decreased as the tilt increased, where after reaching an optimum tilt, the variability again increased, as the axial component does not play a major role in mixing at extremely high tilt resulting in coating non-uniformity. Fig. 8b shows the frequency distribution plot for the same, where a

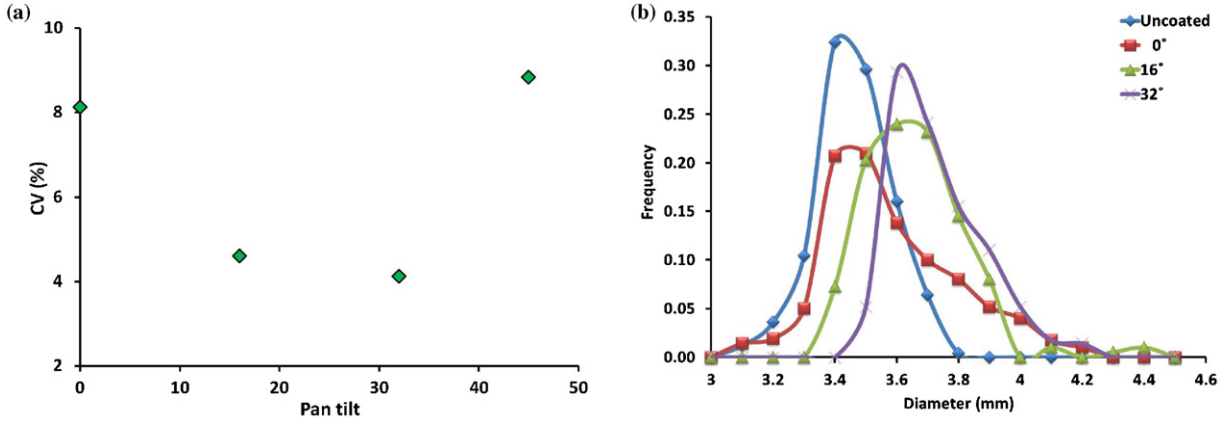

Fig. 8. (a) Effect of pan tilt from horizontal on CV at rotational speed of 30 rpm and FR 6 (2.316 mL/min): 0, 16, 32, and 45. (b) The frequency distribution plot with respect to the change in diameter of the non-pareils for different tilts at 30 rpm and FR 6 (2.316 mL/min).

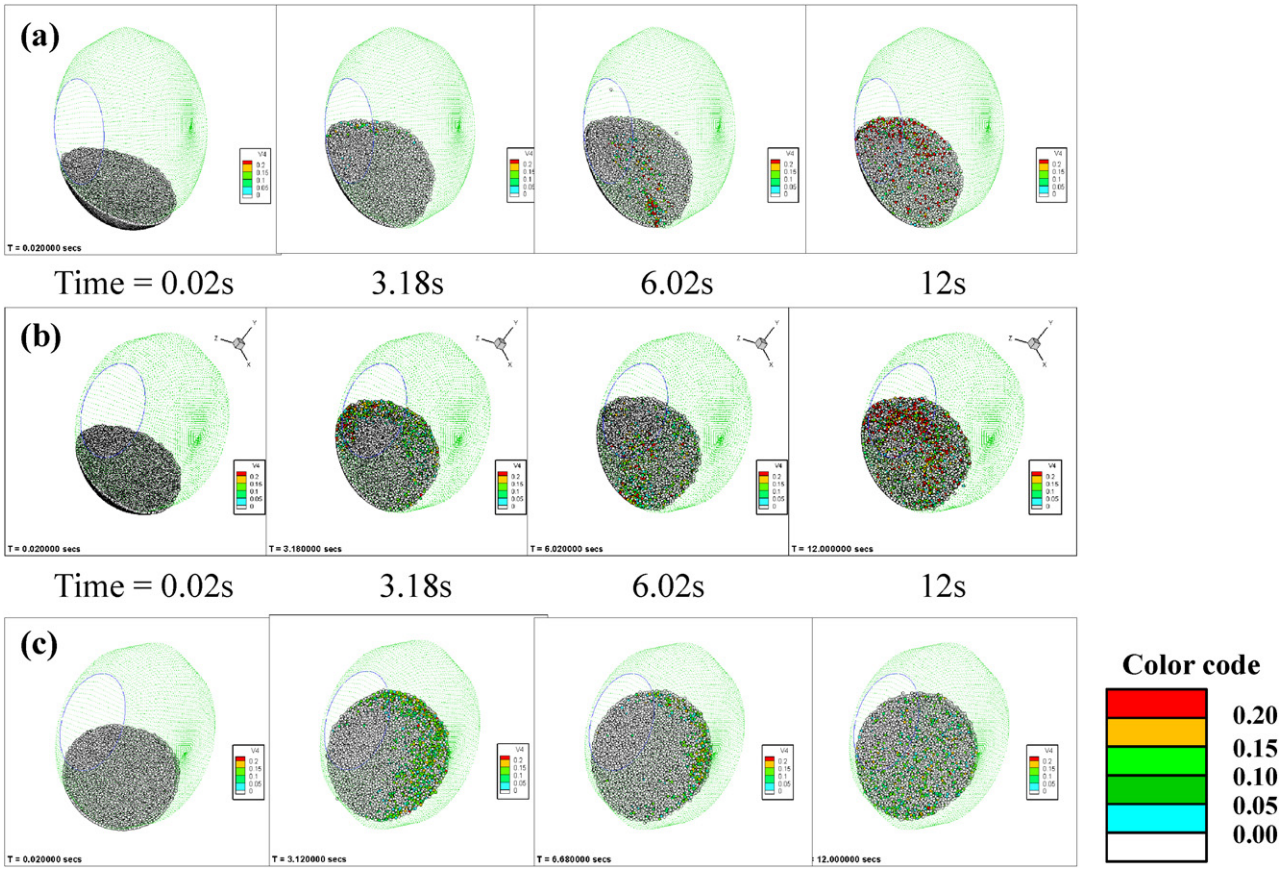

Fig. 9. Simulation results for the effect of Tilt at (a) 0 tilt, (b) 16 tilt, (c) 32 at 1.5 L fill load and 30 rpm where the particles are color coded based on the residence time in the spray.

shift in all the tilts was seen from the uncoated particles. As the tilt increases, the curve becomes more compact approaching towards the Gaussian distribution and hence showing a narrow peak. Therefore, the frequency distribution plot in Fig. 8b further confirms the decrease in variability with increase in tilt upto 32° as compared to 0° and 16° tilt, where the distribution is broad due to wide variation in the particle diameter.

As previously mentioned in Section 2.2, the DEM simulations of coating process were performed using 40,000 spherical particles with the spray duration and interval of 1and 3 s, respectively. The residence time of all the particles were determined by post processing of the particle dynamics data and time spent in the spray zone. The 3D co-ordinates of the centers and radii of the spray zones were determined from the experiments to be used to estimate the residence time distribution.

Time series (T = 0.02, 3.18, 6.02 and 12 s) of snapshots from the coating simulations performed (for 40,000 particles correspond to fill level of 21%) for different vessel orientations (0°, 16°,and 32°) are shown in Figs. 9a–c. The particles were color coded based on the residence time for the simulation where; white shows the uncoated particles, cyan showing particles coated at 0.05 s, green at 0.1 s and red at 0.2 s. The simulation snapshots as shown in Fig. 9, for different tilts depicts that at 0.02 s the particles were uncoated in white and the color begins to develop thereafter. As the tilt increased from 0° to 32°, the coating was more uniform with the decrease in variability of the diameter. At 3.18, 6.02 and 12 s, red color was acquired at

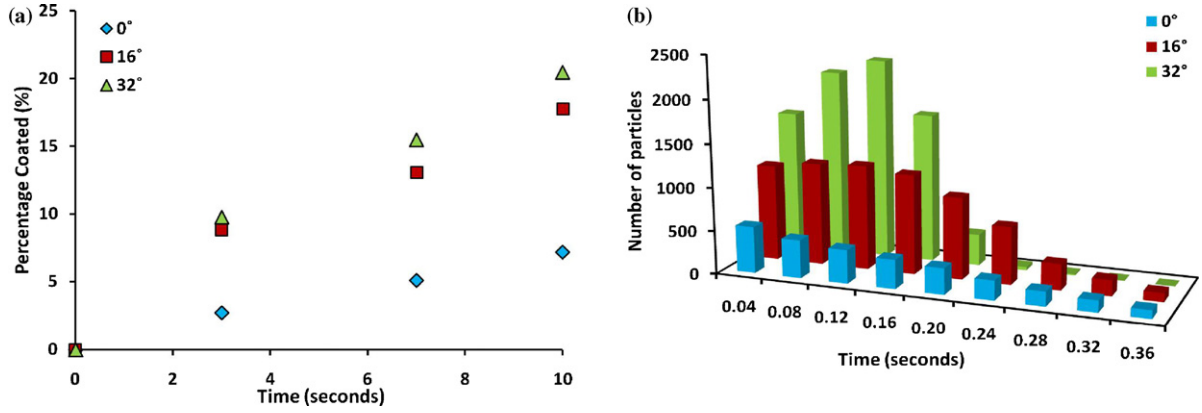

Fig. 10. (a) The simulation results for the effect tilt on percentage coated at pan rotational speed of 30 rpm. (b) The frequency distribution of the residence time of the coated particles for the effect of different tilts at 30 rpm.

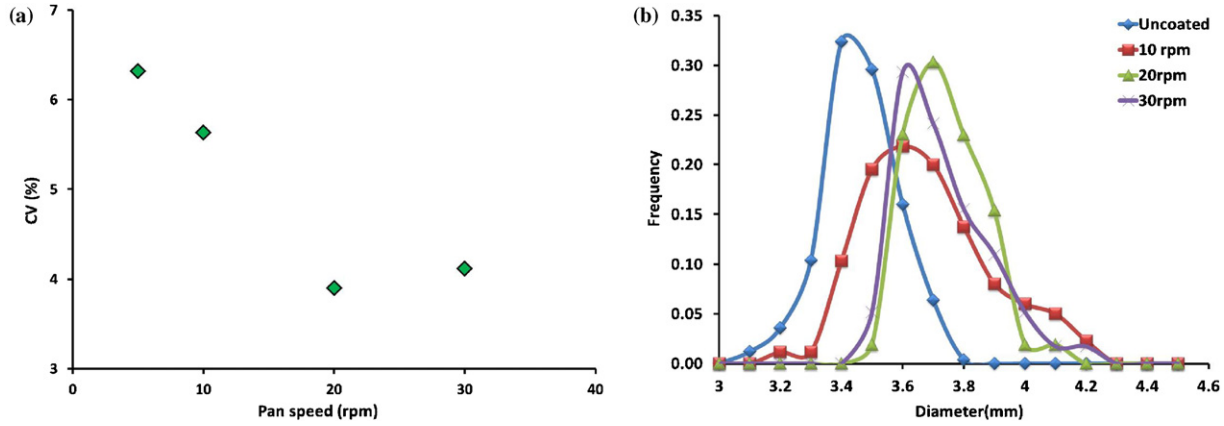

Fig. 11. (a) The effect of different pan speeds on CV at 32 tilt and FR 6 (2.316 mL/min): 5 rpm, 10 rpm, 20 rpm, and 30 rpm. (b) The frequency distribution plot with respect to the change in diameter of the non-pareils for different speeds at 32 tilt and FR 6.

an early stage when coated at 0° tilt showing color non uniformity throughout the bed, resulting due to passage of same non-pareils repeatedly through the spray zone. As shown in Fig. 9a, at 0° tilt the same particles were reintroduced into the spray zone as only radial mixing takes place at horizontal position. But with increase in tilt at 16° and further at 32° as shown in Fig. 9b and c, respectively, the axial component helping in mixing of the bed resulted in more uniform coating of the particles. At 16°tilt, the system is better mixed although still not uniformly. However, Fig. 9c at 32° tilt indicates a uniformly mixed system where green was uniformly distributed throughout the bed showing better mixing and uniform coating at the same tilt. Therefore, the simulation results show uniformity of green color at 32° tilted coater which was in agreement with our experimental findings in Fig. 8a.

The total number of particles passing through the spray zone and the frequency distribution of the residence time of the coated particles were estimated for all orientations of the vessel. Fig. 10a shows the simulation results for the variation of the coated particles with time as a function of vessel tilt. The percentage coated was highest at 32° tilt as compared to the other tilts corroborating that uniform coating was achieved at 32° in less time. Fig. 10b shows the histogram of frequency distribution of the particles. As the tilt increased, the corresponding histogram becomes more compact approaching towards the Gaussian distribution suggesting better

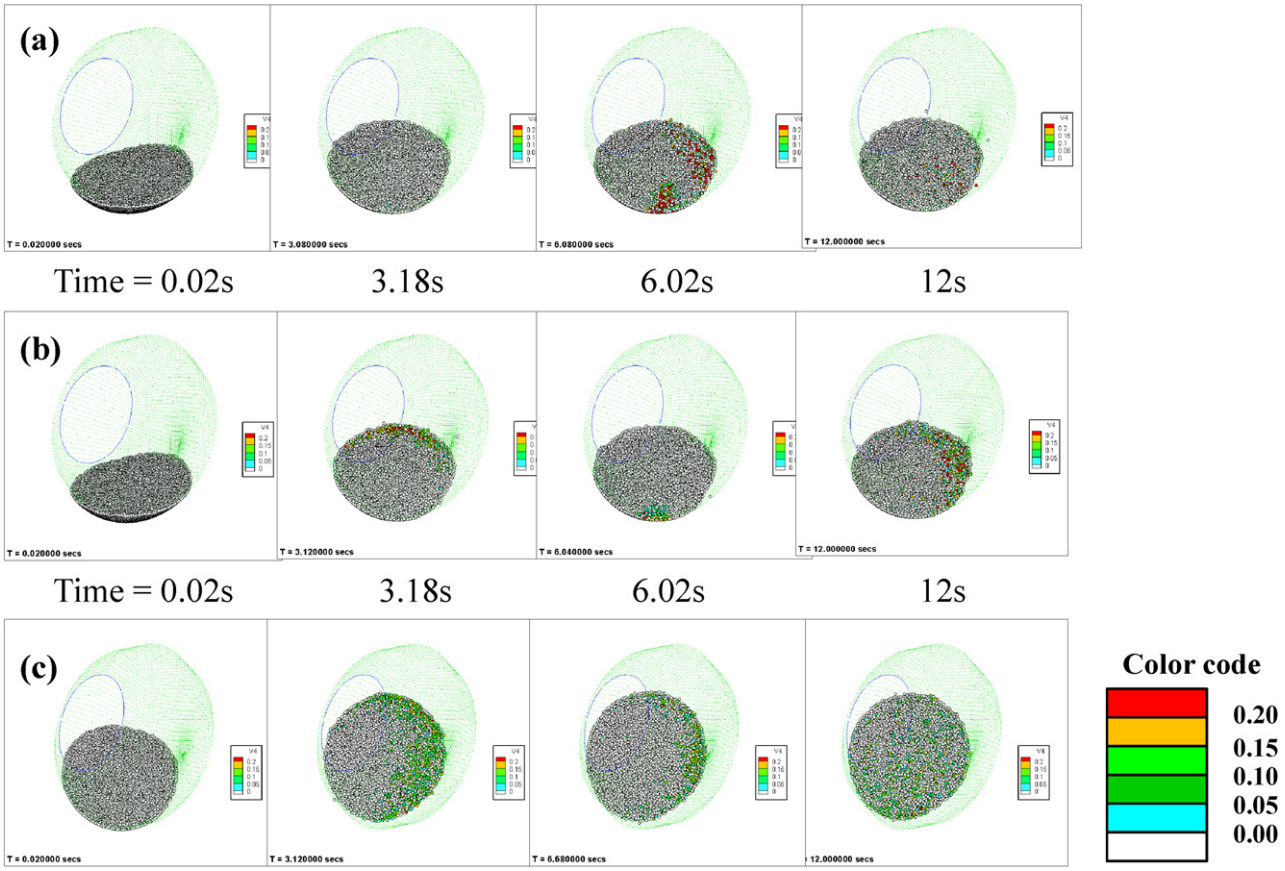

Fig. 12. The snapshots from simulation results for the effect of rotational speed: (a) 10 rpm, (b) 20 rpm, (c) 30 rpm, at 32 tilt for 40,000 particles (1.5 L) with spray duration: 1 s and spray gap: 3 s.

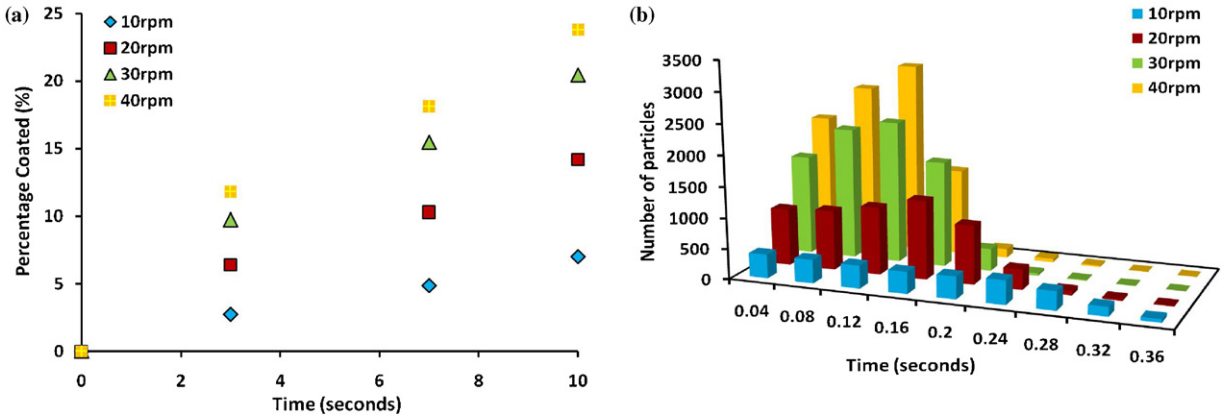

Fig. 13. (a) Effect of rotational speed on coating variability (CV) at 32 tilt. (b) The frequency distribution of the residence time of the coated particles for the effect of speed at 32 tilt.

uniformity. The density of the particles being coated increased with the tilt as the standard deviation decreased with course of time. The simulation snapshots and data were in agreement with the trends observed in the experiments indicating a qualitative validation of the model.

3.2.4. Effect of pan speed on coating variability

Fig. 11a shows the coating variability as a function of time for different pan speeds (5 rpm, 10 rpm, 20 rpm, and 30 rpm). From previous results on mixing, high optimum vessel speed resulted in good mixing of the granular bed thereby improving the coating performance (Sahni et al., 2011). Therefore, the %CV decreased as the pan speed increased. Although on comparing the coating variability with respect to total coating time for 20 and 30 rpm, it is convincing from Figs. 4a and 5a that the variability is less initially for a higher speed though the end effects were similar because with time the variability plateaus to almost the same levels. Frequency distribution plots in Fig. 11b further corroborated the decrease in variability with increase in speed. A wider distribution was observed for 10 rpm, however, the diameter distribution became tighter as the speed increased. Therefore, high pan speeds resulted in better coating uniformity although 20 and 30 rpm did not show any significant difference.

The snapshots of simulation are shown in Fig. 12a–c for different pan rotational speeds: 10 rpm, 20 rpm, and 30 rpm, respectively using post-processed DEM data (for 40,000 particles correspond to fill level of 21%). For visual reasons, the particles were color coded based on their residence time under the spray zone, where white represents the uncoated particles, cyan representing particles coated for 0.05 s, green for particles coated for 0.1 s, yellow for particles coated for 0.15 s, and red for particles coated for 0.2 s. The result in Fig. 12 showed better color uniformity at 30 rpm represented by almost uniform distribution of the green color in Fig. 12c. Hence, uniform coating was observed at the higher optimum operational speed. This is in agreement with our experimental results (Sahni et al., 2011).

The total number of particles passing through the spray zone was estimated from the simulation data and thereafter the frequency distribution of the residence time for the coated particles was calculated. Fig. 13a shows the relation of percentage of coated particles with time for different vessel speeds. The percentage coated was observed to be greater at higher speeds. Fig. 13b shows the corresponding frequency distribution plot. As the vessel speed increased, the histogram approached the bell shaped Gaussian distribution signifying better uniformity of coating as the standard deviation decreased with time. Simulations somewhat over predicted the results for speed as there was not much difference in %CV of 20 and 30 rpm as observed in experiments and 40 rpm would be high enough to break the particles in the experiments.

4. Conclusions

The work presented here was an attempt to develop a mechanistic first principle model to study the coating variability in a pan coater. In the current study, the experimental setup did not reflect the typical bead coating setup used in the industry; rather depict a simplified setup to validate the numerical model. The maximum coating efficiency with minimal variability was accomplished at the optimal coating condition of 32° vessel tilt and rotational speed of 30 rpm, in both experiments and simulations. The coating variability decreased with time under all conditions. The spray flow rate seemed to have a variable effect on coating uniformity. At higher spray concentration, the uniformity increased since coating proceeds in less time with fewer collisions of inter-particle and particle-wall. The trends predicted by the model are consistent with the experimental observations, suggesting that *a priori* predictive tool is developed to assess coating variability based on the assumptions in the text. Hence, the numerical model developed can provide the basis for the adjustments in the process parameters to reduce the coating variability in pan coating process.

Acknowledgements

The authors thank the University of Connecticut Research Foundation (UCRF) for the financial support of this work. We gratefully acknowledge Dr. Robin Bogner for providing the pan coater. We also appreciate the active support of the undergraduates, Yeonsun Choi, Ushma Patel, Robert Yau and Varun Bhattaram in this study.

References

Chang, R.K., Leonzio, M., 1995. Effect of run time on the inter-unit uniformity of aqueous film coating applied to glass beads in a hi-coater. Drug. Dev.Ind. Pharm. 21, 1895–1899.

Cheng, X., Turton, R., 1999. The prediction of variability occuring in fluidized bed coating equipment. II. The role of non-uniform particle coverage as particle pass through the spray zone. Pharm. Dev. Technol. 5, 323–332.

Denis, C., Hemati, M., Chulia, D., Lanne, J.Y., Buisson, B., Daste, G., Elbaz, F., 2003. A model of surface renewal with application to the coating of pharmaceutical tablets in rotary drums. Powder Technol. 130, 174–180.

Fourman, G.L., Hines, C.W., Hritsko, R.S., 1995. Assessing the uniformity of aqueous film coatings applied to compressed tablets. Pharm. Technol. 19, 70, 72, 74, 76.

Joglekar, A., Joshi, N., Song, Y., Ergun, J., 2007. Mathematical model to predict coat weight variability in a pan coating process. Pharm. Dev. Technol. 12, 297–306.

Kalbag, A., Wassgren, C., Penumetcha, S.S., Pérez-Ramos, J., 2008. Inter-tablet coating variability: residence times in a horizontal pan coater. Chem. Eng. Sci. 63, 2881–2894.
Kalbag, A., Wassgren, C., 2009. Inter-tablet coating variability: tablet residence time variability. Chem. Eng. Sci. 64, 2705–2717.
Khakhar, D., McCarthy, J., Shinbrot, T., Ottino, J., 1997. Transverse flow and mixing of granular materials in a rotating cylinder. Phys. Fluids. 9, 31–43.
Kushaari, K., Pandey, P., Song, Y., Turton, R., 2006. Monte Carlo simulation to determine coating uniformity in a Wurster fluidized bed coating process. Powder Technol. 166, 81–90.
Leaver, T.M., Shannon, H.D., Rowe, R.C., 1985. A photometric analysis of tablet movement in a side-vented perforated drum (Accela-Cota). J. Pharm. Pharmacol. 37, 17–21.
Mann, U., 1983. Analysis of spouted-bed coating and granulation. I. Batch operation. Ind. Eng. Chem. Proc. Des. Dev. 22, 288–292.
Mishra, B.K., Rajamani, R.K., 1992. The discrete element method for the simulation of ball mills. Appl. Math. Model. 16, 598–604.
Moakher, M., Shinbrot, T., Muzzio, F.J., 2000. Experimentally validated computations of flow, mixing and segregation of non-cohesive grains in 3D tumbling blender. Powder Technol. 109, 85–94.
Nakamura, H., Abe, E., Yamada, N., 1998. Coating mass distribution of seed particles in a tumbling fluidized bed coater. Part 2. Monte Carlo simulation of particle coating. Powder Technol. 99, 140–146.
Pandey, P., Katakdaunde, M., Turton, R., 2006a. Modeling weight variability in a pan coating process using Monte Carlo simulations. AAPS Pharm. Sci. Technol. 7, E1–E10.
Pandey, P., Song, Y., Kahiyan, F., Turton, R., 2006b. Simulation of particle movement in a pan coating device using discrete element modeling and its comparison with video-imaging experiments. Powder Technol. 161, 79–88.
Prater, D.A., Wilde, J.S., Meakin, B.J., 1980. A model system for the production of aqueous tablet film coatings for laboratory evaluation. J. Pharm. Pharmacol. 32S, 90.
Rothenburg, L., Bathurst, R.J., 1992. Micromechanical features of granular assemblies with planar elliptical particles. Geotechnique 42, 79–95.
Sahni, E., Yau, R., Chaudhuri, B., 2011. Understanding granular mixing to enhance coating performance in a pancoater: experiments and simulations. Powder Technol. 205, 231–241.
Sandadi, S., Pandey, P., Turton, R., 2004. In situ, near real-time acquisition of particle motion in rotating pan coating equipment using imaging techniques. Chem. Eng. Sci. 59, 5807–5817.
Sherony, D.F., 1981. A model of surface renewal with application to fluid bed coating of particles. Chem. Eng. Sci. 36, 845–848.
Skultety, P.F., Rivera, D., Dunleavy, J., Lin, C.T., 1988. Quantitation of the amount and uniformity of aqueous film coating applied to tablets in a 24″ Accela-Cota. Drug. Dev. Ind. Pharm. 14, 617–631.
Strack, O.D., Cundall, P.A., 1979. A discrete numerical model for granular assemblies. Geotechnique 29, 47–65.
Tobiska, S., Kleinebudde, P., 2001. A simple method for evaluating the mixing efficiency of a new type of pan coater. Int. J. Pharm. 224, 141–149.
Turton, R., 2008. Challenges in the modeling and prediction of coating of pharmaceutical dosage forms. Powder Technol. 181, 186–194.
Walton, O., Braun, R., 1986. Viscosity, granular-temperature and stress calculations for shearing assemblies of inelastic, frictional disks. J. Rheol. 30, 949–980.
Walton, O.R., Braun, R.L., 1993. Proceedings of the Joint DOE/NSF Workshop on the Flow of Particulates and Fluids, 29 September–1 October, 1993 , Ithaca, New York, pp. 131–148.
Yamane, K., Sato, T., Tanaka, T., Tsuji, Y., 1995. Computer simulation of tablet motion in coating drum. Pharm. Res. 12, 1264–1268.